第34卷第2期　　红外与毫米波学报　　Vol. 34, No. 2
2015年4月　　J. Infrared Millim. Waves　　April, 2015

文章编号: 1001－9014(2015)02－0134－06　　DOI:10.11972/j.issn.1001－9014.2015.02.002

Resonant IR detectors based on microbridge resonators electrothermally excited and piezoresistively detected using polysilicon resistors of negative TCR

HAN Jian-Qiang, LI Sen-Lin, LI Yan, WANG Xiao-Fei, FENG Ri-Sheng

(College of Mechanical and Electrical Engineering, China Jiliang University, Hangzhou 310018, China)

Abstract: A novel type resonant infrared (IR) detector based on microbridge resonators electrothermally excited and piezoresistively detected using polysilicon resistors of negative temperature coefficient of resistance (TCR) was presented. The temperature rise of microbridges due to absorbed infrared radiation reduces the resistance of the excitation resistors and Wheatstone bridges. As a result, both the static component of the exciting power and the Joule heat of Wheatstone bridges accordingly increase with reducing the resistance. It is equivalent to increasing infrared radiation power. From preliminary experimental results, the feasibility of sensing infrared radiation is demonstrated.

Key words: microbridge resonator, IR detector, polysilicon resistor, negative temperature coefficient of resistance
PACS: 07.57.Kp

基于负温度系数的多晶硅电阻电热激励/压阻检测微桥谐振器的新型红外探测器

韩建强, 李森林, 李 琰, 王小飞, 冯日盛
(中国计量学院 机电工程学院,浙江 杭州 310018)

摘要:报道了一种基于负电阻温度系数的多晶硅电阻电热激励/压阻检测 $SiO_2/Si_3N_4/Si_xN_y$ 微桥谐振器的新型红外探测器.微桥谐振器吸收的红外辐射引起微桥温度升高,激励电阻和检测电桥的阻值减小,使得恒定激励电压作用下激励电阻的静态功率和惠斯登电桥的焦耳热增加,等效于增加了辐射在微桥谐振器上的红外辐射.初步的实验证实了该方案的可行性.

关 键 词:微桥谐振器;红外探测器;多晶硅电阻;负电阻温度系数
中图分类号:TN215; TN605　　**文献标识码**:A

Introduction

Infrared detectors have been widely used for temperature measurement especially at high temperature and/or noncontact measurements, calorimeters, night vision, electrical equipment, hot spot identification, imaging, chemical and biological applications etc. It is well known that IR detectors can be classified into two types, photodetectors and thermal detectors. Photodetectors exhibit a higher responsivity and detectivity than that of thermal detectors. However, expensive and unwieldy cooling systems are usually required for using photodetectors because of the small band gap of semiconductor materials used in photodetectors.

Thermal detectors are advantageous, as they are capable of operating at room temperature. Various thermal IR sensors have been reported, such as bolometers [1], pyroelectric detectors [2-3], golay cells [4], silicon diodes [5] and microcantilevers [6]. These low-cost IR detectors can be used in nonmilitary applications, such as gas detection, target identification, high temperature and/or noncontact measurements and so on. With the development of above-mentioned thermal IR sensors providing analog signals, resonant IR sensors are gradually attracting more and more attention because the output frequency signal can be measured with the best accuracy and long distance transferred without distortion.

The most reported resonant IR detectors are quartz

Received date: 2013-09-05, **revised date**: 2015-02-06　　**收稿日期**: 2013-09-05, **修回日期**: 2015-02-06
Foundation items: Supported by National Natural Science Foundation of China (61076110), and Supported by Zhejiang Key Discipline of Instrument Science and Technology(JL130101).
Biography: HAN Jian-Qiang(1970-), male, Professor. Research area is MEMS and microsensors. E-mail: hjqsmx@sina.com

resonators [7-11]. An important reason that quartz resonators are used for IR detection is that quartz resonators are among the lowest-noise devices known. The frequencies of the lowest-noise quartz resonators can be measured with a precision of 14 significant figures [12]. But the temperature sensitivities of AC, SC (dual mode), Z, and Y-Cut quartzes are only-20, $-80 \sim 100$, -85, -90 ppm/K, respectively [13-14]. The low temperature sensitivities limit the improvement of responsivity and detectivity. In addition, quartzes are difficult to be thinned. It makes the response time of quartz IR detectors larger than that of other thermal IR detectors.

Another type of resonant IR detectors is based on micromechanical resonators. Micromechanical resonators are extremely popular as ultra-sensitive sensors for sensing mass, acceleration, pressure, fluids flow, and specific chemical or biological agents. The use of micromechanical resonators for detecting infrared radiation is a natural extension of these applications. C. Cabuz proposed the first micromechanical resonant IR detector in 1993[15]. A microbeam resonator was clamped on a silicon frame of which one-side was bonded to the glass in order to avoid package stresses. The microbeam resonator consisted of a P^{++} silicon absorber supported with a thin silicon dioxide beam from the silicon frame. The silicon dioxide beam isolated P^{++} silicon from the silicon frame not only electrically but also thermally. Vibration of the microbeam was driven electrostatically and detected capacitively. However, the large compressive stress of silicon dioxide inevitably buckled the microbeam resonator. Takahito Ono presented another resonant IR detector with the capability of de-amplifying thermal noises in 2005[16]. A crystalline silicon cantilever resonator was formed at the edge of an absorber that was freely suspended by narrow beams. The resonance frequency of the resonator was changed by both heat conduction and thermal stress upon irradiating IR radiation. An electrode for electrostatically vibrating was integrated, and two electrodes for electrostatically exciting parametric amplification were also formed near the resonator. The frequency fluctuation of the mechanical vibration could be reduced by noise-squeezing involved in parametric amplification under an appropriate condition, resulting in improvement of the noise equivalent power and normalized detectivity. Mina Rais-Zadeh reported a low-noise un-cooled infrared detector using a combination of piezoelectric, pyroelectric, electrostrictive, and resonant effects in 2012[17]. The architecture consisted of a parallel array of high-Q gallium nitride microresonators coated with an IR absorbing nanocomposite. The nanocomposite absorber converted the IR energy into heat with high efficiency. The generated heat caused a shift in frequency characteristics of the GaN resonator because of pyroelectric effect. The resonance frequency of a prototype GaN resonator was 119.23 MHz and the shift of resonant frequency was found to be approximately 21.8 KHz upon irradiation with 56 μW of IR power.

1 Fabrication progress of infrared detectors

In this paper, a novel type of resonant IR detectors based on microbridge resonators electrothermally excited and piezoresistively detected by polysilicon resistors of negative temperature coefficient of resistance (TCR) is presented. The main part of a micromechanical resonant IR detector is two simple microbridge resonators with rectangular cross section on a chip. Both ends of microbridges are clamped on the silicon substrate. The microbridge resonators consists of 0.92 μm silicon dioxide film, 0.21 μm silicon nitride film deposited by low pressure chemical vapor deposition (LPCVD) process and 0.65 μm silicon nitride film deposited by plasma-enhanced chemical vapor deposition (PECVD) process. The residual stress of SiO_2 film, LPCVD Si_3N_4 film, PECVD Si_xN_y film is-300 MPa, 740 MPa and 402 MPa, respectively. The compressive stress of silicon dioxide film is compensated by the tensile stress of silicon nitride films. The original tensile strain can avoid the buckle of microbridges under the action of thermal stress due to constant component of the exciting power, Joule heat of piezoresistive Wheatstones and absorbed infrared radiation. Both the silicon dioxide film and the silicon nitride film have the largest width of absorption peak between 8 μm and 12 μm [18-19], which make them well suited for the absorber of IR detectors.

The process sequence of the resonant IR detectors starts from (100) oriented, n-type silicon wafers of $3 \sim 6\ \Omega$ resistivity. The main process flow is as follows.

(1) A silicon dioxide film of thickness 0.92 μm is thermally grown on both sides of the wafers at 1 100 ℃.

(2) A silicon nitride film of thickness 0.21 μm and a polysilicon film of thickness 0.8 μm are deposited on both sides of the wafers by low pressure chemical vapor deposition process.

(3) Boron ions are implanted in polysilicon film at the front side of wafers. The implantation energy is 30 KeV and the dose is $1.5 \times 10^{15}\ cm^{-2}$. The implanted boron atoms are activated by thermal annealing process at 950 ℃.

(4) The polysilicon film at the backside of wafers is etched in TMAH solution. The P^{+} polysilicon film at the front side of wafers is patterned and etched to form excitation resistors at the middle of microbridges and Wheatstone bridges at the clamped ends.

(5) Si_xN_y film of thickness 0.65 μm is deposited by plasma-enhanced chemical vapor deposition process on the front side of wafers using pure NH_3 and 5% SiH_4. The flow of NH_3 and 5% SiH_4 are 30 sccm and 45 sccm, respectively. The RF power, substrate temperature and pressure are kept at 80 W, 350 ℃ and 32 Pa, respectively. The residual stress of the PECVD silicon nitride films is measured to be 402 MPa by Dektak 150 surface profiler.

(6) Electrical contact holes are patterned. An aluminum film of thickness 0.8 μm is deposited on the front side of wafers by sputtering and patterned for the electrical connection.

(7) The microbridges are patterned at the front side of wafers along the 〈110〉 direction. The silicon nitride films and silicon dioxide film in the slots defining microbridges are etched by dry etching.

(8) Windows below microbridge resonators are patterned at the backside of the wafer. Anisotropic wet etching through the windows is carried out in KOH solution in

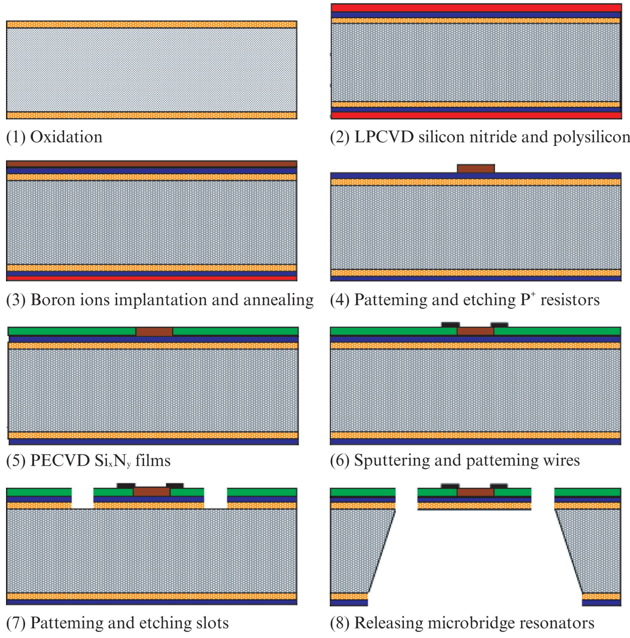

Fig. 1 The fabrication process for resonant IR detectors based on microbridge resonators
图 1 基于微桥谐振器的谐振式红外探测器的制作工艺流程

order to thin wafers to 30 μm, while protecting the front side in a mechanical chuck. Then microbridge resonators are released by deep reactive ion etching process.

A fabricated microbridge resonator is shown in figure. 2. The length and width of the microbridge are 500 μm and 110 μm, respectively. The sensor chip is bonded on a graphite sheet of 1 mm thickness with thermally conductive adhesive. Graphite has a thermal expansion coefficient approximately equal to that of silicon and good thermal conductivity. Then it is glued in a metal packaging. Bonding wire connects pads on the chip to lead electrodes on the metal packaging.

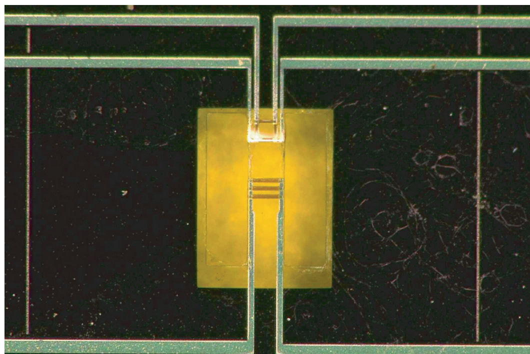

Fig. 2 Photograph of a $SiO_2/Si_3N_4/Si_xN_y$ microbridge resonator electrothermally excited and piezoresistively detected by polysilicon resistors of negative temperature coefficient of resistance
图 2 基于负温度系数的多晶硅电阻电热激励/压阻检测微桥谐振器

2 Responsivity of the resonant IR detector

If the vibration amplitude (W_{max}) of a microbridge resonator is much less than the radius of gyration, the non-linear effects can be ignored and the first-order resonance frequency of the microbridge resonator is [20]

$$f_1(\varepsilon)=\frac{\alpha_1^2 h}{2\pi\sqrt{12}L^2}\sqrt{\frac{E}{\rho(1-\nu^2)}}\sqrt{1+\gamma_1\varepsilon(1-\nu^2)\left(\frac{L}{h}\right)^2}\quad,(1)$$

here $\alpha_1=4.732$, $\gamma_1=0.2949$. L, h and ε are the length, thickness and axial strain of the microbridge. ν, E and ρ are poisson's ratio, equivalent Young's modulus and density of the material. The responsivity of the microbridge resonator to the absorbed infrared power (P_3) can be calculated as

$$\frac{df_1(\varepsilon)}{f_1 dP_3}=\frac{\gamma_1(1-\nu^2)\left(\frac{L}{h}\right)^2}{2\left[1+\gamma_1\varepsilon(1-\nu^2)\left(\frac{L}{h}\right)^2\right]}\frac{d\varepsilon}{dP_3}\ .(2)$$

Assumed that the length between two clamped ends keep constant, the axial strain of a microbridge can be as expressed below

$$\varepsilon=\varepsilon_0-\bar{\alpha}\Delta T_{av}=\varepsilon_0-\bar{\alpha}(\Delta T_{av1}+\Delta T_{av2}+\Delta T_{av3})\quad,(3)$$

where ε_0 is original axial strain of the microbridge resonator produced in the fabrication process. ΔT_{av1}, ΔT_{av2} and ΔT_{av3} are the average temperature rise of the microbridge due to static component (P_1) of the exciting power, Joule heat (P_2) of Wheatstones and absorbed infrared power (P_3).

Assumed that the substrate is an ideal heat sink, the absorbed infrared power (P_3) results in a static temperature rise in the microbridge [21].

$$\Delta T_3(x)=\frac{P_3(L/2-|x|)^2}{4L\sum b_i\lambda_i h_i}\quad,\quad(4)$$

here the grid origin of coordinate system locates at the midpoint of the microbridge. b_i, h_i and λ_i are the width, thickness and thermal conductivity of thin films constituting the microbridge, respectively. The average temperature rise relative to the substrate can be calculated as

$$\Delta T_{av3}=\frac{1}{L}\int_{-L/2}^{L/2}\Delta T_3(x)dx=\frac{P_3 L}{48\sum b_i\lambda_i h_i}\ .(5)$$

The equivalent thermal expansion coefficient of the microbridge can be calculated as

$$\bar{\alpha}=\frac{\sum\alpha_i E_i h_i}{\sum E_i h_i}\quad,\quad(6)$$

α_i and E_i are the thermal expansion coefficient and Young's modulus of thin films, respectively.

The derivative of axial strain with respect to the absorbed infrared power (P_3) can be found from Eq. 3, 5–6 as

$$\frac{d\varepsilon}{dP_3}=-\bar{\alpha}\frac{d(\Delta T_{av})}{dP_3}=-\frac{\sum\alpha_i E_i h_i}{\sum E_i h_i}\frac{L}{48\sum b_i\lambda_i h_i}\ .(7)$$

Substituting Eq. 7 into Eq. 2, we find the responsivity of the microbridge resonator to the absorbed infrared power

$$\frac{df_1(\varepsilon)}{f_1 dP_3}=-\frac{\gamma_1(1-\nu^2)}{96h^2\left[1+\gamma_1\varepsilon(1-\nu^2)\left(\frac{L}{h}\right)^2\right]}\frac{\sum\alpha_i E_i h_i}{\sum E_i h_i}\frac{L^3}{\sum b_i\lambda_i h_i}\ .\quad(8)$$

It can be seen from Eq. 8 that the resonance frequency of

microbridge resonators decreases with absorbed infrared power.

In above calculations, the temperature coefficient of resistance hasn't been taken into account. In fact, the temperature rise of microbridges due to absorbed infrared power reduces the resistance (r) of the excitation resistors with negative temperature coefficient of resistance. The static component of the exciting power ($u_{ac}^2/2r$) under harmonic ac voltage ($u_{ac}\cos\omega t$) accordingly increases with reducing the resistance of excitation resistors. It can also increase the temperature of microbridges. As a result, the responsivity of novel IR detectors is improved for negative temperature coefficient of resistance. Since the static component of the exciting power is in the order of milliwatts, which is 2 ~ 3 orders of magnitude larger than absorbed infrared power, a small amount change in exciting power will cause large change of resonance frequency. It is equivalent to a substantial increase of the absorbed infrared power.

Similarly, the temperature rise of microbridges due to absorbed infrared power will also reduce the resistance of the Wheatstone bridges at the clamped ends. As a result, the Joule heat increases and the resonance frequency reduces under constant DC voltage applied to the Wheatstone bridge. It is also equivalent to increasing the absorbed infrared power.

The increased static component of the exciting power and Joule heat will further heat microbridges. The absorbed infrared power, the static component of the exciting power, Joule heat, heat conduction to the package and heat convection to air determine the final temperature distribution and resonance frequency of microbridges. The complicated mechanism of this resonant IR detector is illustrated in Fig. 3

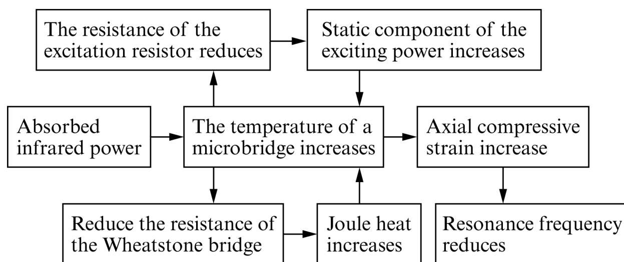

Fig. 3　The mechanism of resonant IR detectors based on microbridge resonators electrothermally excited and piezoresistively detected by polysilicon resistors of negative temperature coefficient of resistance

图 3　基于负温度系数多晶硅电阻电热激励/压阻检测微桥谐振器的红外探测器的工作机制

3　Results and discussion

3.1　The temperature coefficient of polysilicon resistors

Before measuring the detective characteristics of novel IR detectors, the temperature coefficient of the excitation resistors, Wheatstone bridges and resistors on the substrate is measured. An IR detector is placed in a constant temperature oven. The resistance of the excitation resistor, Wheatstone bridge and a resistor on the substrate measured at different temperature is shown in Fig. 4. The temperature coefficients of three resistors are calculated to be -2.22×10^{-3}/℃, -1.188×10^{-3}/℃ and -1.42×10^{-3}/℃, respectively. As shown in Fig. 4, the resistance of polysilicon resistors reduces with increasing ambient temperature.

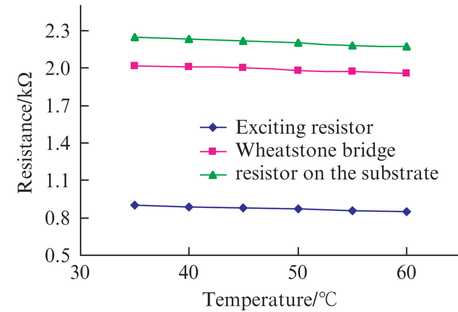

Fig. 4　Temperature dependence of the excitation resistor, Wheatstone bridge and resistor on the substrate

图 4　激励电阻、惠斯通电桥和衬底电阻的温度特性

3.2　The frequency response of microbridge resonators to infrared radiation

The experimental setup for measuring the frequency response of microbridge resonators to infrared radiation is shown in Fig. 5. An infrared thin film radiation source (JSIR350-22-R) is positioned close to the sensor at a distance of approximately 21.7 mm. The off and on of the infrared thin film radiation source is controlled by a 50% duty-cycle square wave with a period of 10 seconds through a triode (8 550). The full wavelength IR power density at the sensor position is approximately calculated to be 185.49 μW/mm^2. As a result, the full wavelength IR power irradiating the microbridge resonator with a size of 500 × 110 μm^2 is 10.2 μW.

To measure the frequency response of a bridge resonator to infrared radiation, it is self-oscillated near the resonance using a closed-loop circuit depicted in previous literature [22]. The amplitude of AC exciting voltage applied to the excitation resistor is about 1 V and the DC voltage applied to the Wheatstone bridge is 3 V. The output resonance frequency of closed-loop self-exciting circuit is measured by Agilent 34 401 multimeter and sent to a virtual frequency meter programmed by labview through RS232 serial communication.

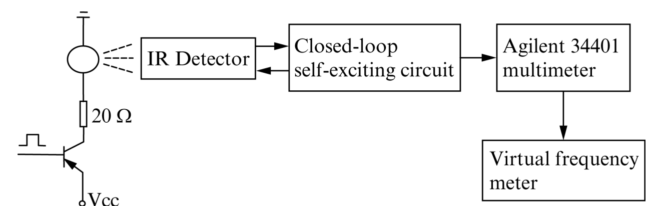

Fig. 5　The experimental system for measuring the frequency response of resonators to infrared radiation

图 5　红外探测特性测试系统

Figure 6 (a) shows the frequency response of the microbridge resonator upon IR irradiation. The shift of resonant frequency is −20.8 Hz upon IR radiation of 10.2 μW. The responsivity of the microbridge resonator to the absorbed infrared power can be calculated as

−15.71 ppm/μW. It is about 27% of the theoretic prediction value (−58.66 ppm/μW) calculated from Eq. 8. The geometry and physical characteristics of films used in calculating are summarized in table. 1 The reason for this deviation is that the peak wavelength of infrared radiation source is 3.5 μm, while the silicon dioxide film and the silicon nitride film have the largest width of absorption peak between 8 μm and 12 μm.

Table 1 The geometry and physical characteristics of films
表1 薄膜的结构尺寸与物理特性

Films	Thickness	Width	Young's Modulus	Thermal Conductivity	Thermal Expansion Coefficient
SiO_2	0.92 μm	110 μm	0.67×10^{11} N/m^2	1.113 W/m·K	0.25×10^{-6}/℃
Si_3N_4	0.21 μm	110 μm	3.2×10^{11} N/m^2	3 W/m·K	3×10^{-6}/℃
Si_xN_y	0.65 μm	110 μm	1.78×10^{11} N/m^2	3.25 W/m·K	3×10^{-6}/℃
Al	0.8 μm	10 μm	—	146 W/m·K	—

Figure 6 (b) shows the resonance frequency (f_2) of a reference microbridge resonator on the same chip, which has not been radiated with infrared ray. The fluctuation of the resonance frequency is only (1 Hz. The responsivity ($(f_2-f_1)/f_2P_3$) of the beat frequency (f_2-f_1) is about −1 204.5 ppm/μW.

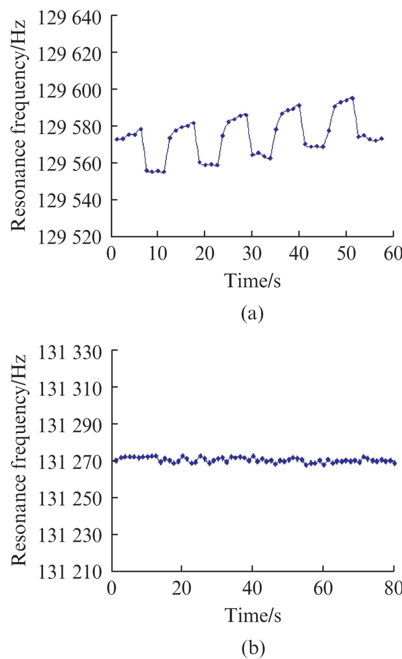

Fig. 6 (a) The frequency response of the microbridge resonator upon irradiation; (b) The frequency fluctuate of a reference resonator on the same chip
图6 (a)微桥谐振器对红外辐射的频率响应;(b)同一芯片上参考谐振器的频率波动

3.3 Temperature dependence of the resonant frequency

For an ideal IR detector, its temperature sensitivity should be as small as possible. Figure 7 shows the measured frequency change of the microbridge resonator against the ambient temperature. From this curve, the temperature sensitivity of 16.8 Hz/℃ is obtained, which corresponds to the temperature coefficient of resonance frequency of 127.17 ppm/℃. Reducing the temperature drift is the following task to develop this kind of resonant IR detectors.

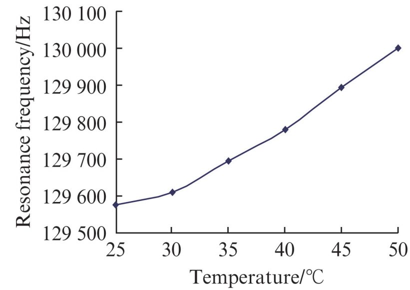

Fig. 7 The resonance frequency dependence of the resonator upon the ambient temperature
图7 谐振器在不同环境温度下的谐振频率

4 Conclusions

A resonant IR detector based on microbridge resonators electrothermally excited and piezoresistively detected with polysilicon resistors of negative TCR is proposed and its feasibility is demonstrated. Although the responsivity of this type IR detector is smaller than that of theoretical predictions, we expect that larger responsivity can be achieved by optimizing the sensor structure and packaging. We are now striving to design new structure of bridge resonators to avoid package stresses and improve the responsivity and detectivity of IR detectors.

References

[1] Dobrzanski L, Nowak Z, Piotrowski J. Micromachined silicon bolometers as detectors of soft X-ray, ultraviolet, visible and infrared radiation [J]. *Sensors and Actuators. A*, 1994, **60**(1-3): 154-159.

[2] Belcher J F, Hanson C M, Beratan H R. Uncooled monolithic ferroelectric IR FPA technology [J]. *Proceedings of SPIE*, 1998, **3436**: 611-622.

[3] Völklein F, Wiegand A, Baier V. High sensitivity radiation thermopile made of Bi-Sb-Te films [J]. *Sensors and Actuators. A*, 1991, **29**(2): 87-91.

[4] Kenny T W, Kaiser W J, Waltman S B. Novel infrared detector based on a tunneling displacement transducer [J]. *Appl. Phys. Lett*, 1991, **59**(15): 1820-1822.

[5] Kim J K, Han C H. A new uncooled thermal infrared detector using silicon diode [J]. *Sensors and Actuators. A*, 2001, **89**(1-2): 22-27.

[6] Barnes J R, Stephenson R J, Woodburn C N. A femtojoule calorimeter using micromechanical sensors [J]. *Rev. Sci. Instrum*, 1994, **65**(12): 3793-3798.

[7] Hamrour M R, Galliou S, Dulmet B. A new type of infrared-sensitive resonator used as a thermal sensor [J]. *Sensors and Actuators A*, 1998, **65**(2-3): 147-151.

[8] Pisani M B, Kao P, Tadigadapa S. Bulk acoustic wave resonators for infrared detection applications [J]. Transducers 2009, Denver, CO, USA, June 21-25, 2009: 1959-1962.

[9] Kim Y, Vig J R. Experimental results on a quartz microresonator IR sensor [J]. *IEEE Ultrasonics Symposium*. 1, 1997: 449-453.

[10] Tsow F, and Tao N J. Microfabricated tuning fork temperature and infrared sensor [J]. *Applied Physics Letters*, 2007, **90**(17): 174102-174102-3.

[11] Kao P, Tadigadapa S. Micromachined quartz resonator based infrared detector array [J]. *Sensors and Actuators. A*, 2009, **149**(2): 189-

192.
[12] Walls F L, and Vig J R. Fundamental limits on the frequency stabilities of crystal oscillators[J]. *IEEE Transactions on Ultrasonics, Ferroelectrics and Frequency Control*, 1995, **42**(4): 576 - 589.
[13] Ralph J E, King R C, Curran J E, *et al*. Miniature quartz resonator thermal detector[J]. *IEEE Ultrasonics Symposium*. 1, 1985: 362 - 364.
[14] Hamrour M R, Galliou S, Dulmet B. A new type of infrared-sensitive resonator used as a thermal sensor[J]. *Sensors and Actuators A Phys*, 1998, **65**(2 - 3): 147 - 151.
[15] Cabuz C, Shoji S, Fukatsu K, *et al*. Sensitive resonant sensor[J]. *Proc. Transducers'93, Yokohama*, 1993: 694 - 697.
[16] Ono T, Wakamatsu H, Esashi M. Parametrically amplified thermal resonant sensor with pseudo-cooling effect[J]. *J. Micromech. Microeng*, 2005, **15**(12): 2282 - 2288.
[17] Rais-Zadeh M. Gallium nitride micromechanical resonators for IR detection[J]. *Invited Paper, Proc. SPIE*, April. 2012: 8387 - 83731M - 1.
[18] Fourmond D J, Lelièvre J F. Impact of PECVD SiON stoichiometry and post-annealing on the silicon surface passivation[J]. *Thin Solid Films*, 2008, **516**(20): 6954 - 6958.
[19] Ono H, Ikarashi T, Miura Y. Bonding configurations of nitrogen absorption peak at 960 cm^{-1} in silicon oxynitride films[J]. *Applied Physics Letters*, 1999, **74**(2): 203 - 205.
[20] Tilmans H A C, Elwenspoek M, Fluitman J H J. Micro resonant force gauges[J]. *Sensors and Actuators A*, 1992, **30**(1 - 2): 35 - 53.
[21] Liu Y M, Liu J H, Zhang S J. The performance and optimization of the silicon bi-material cantilever excited by light and heat[J]. *Journal of Functional Materials and Devices*, 2000, **6**(1): 19 - 24.
[22] Han J Q, Song M X, Wang X F, *et al*. Dependence of the resonance frequency of mircobridge resonators on the thermal power and vacuum [J]. *Advanced materials Research*, 2012, **465**: 14 - 22.